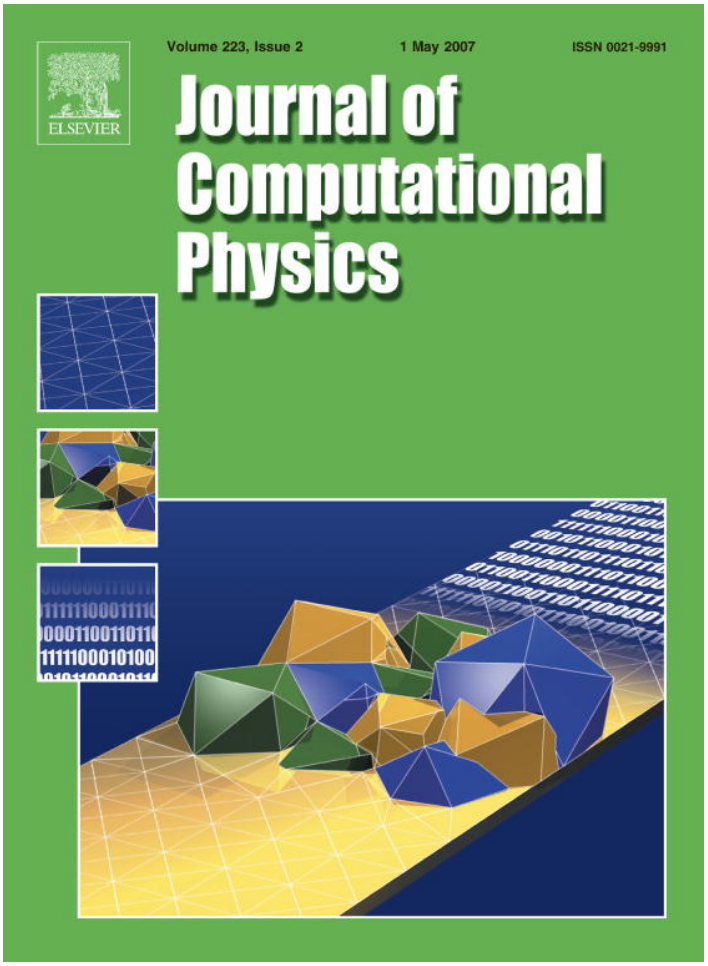

Available online at www.sciencedirect.com
ScienceDirect
Journal of Computational Physics 223 (2007) 774–782
JOURNAL OF COMPUTATIONAL PHYSICS
www.elsevier.com/locate/jcp

The use of bulk states to accelerate the band edge state calculation of a semiconductor quantum dot ☆

Christof Vömel [a,*], Stanimire Z. Tomov [b], Lin-Wang Wang [a], Osni A. Marques [a], Jack J. Dongarra [b]

[a] *Computational Research Division, Lawrence Berkeley National Laboratory, Berkeley, CA 94720, United States*
[b] *Computer Science Department, University of Tennessee, Knoxville, TN 37996-3450, United States*

Received 10 May 2006; received in revised form 3 August 2006; accepted 3 October 2006
Available online 17 November 2006

Abstract

We present a new technique to accelerate the convergence of the folded spectrum method in empirical pseudopotential band edge state calculations for colloidal quantum dots. We use bulk band states of the materials constituent of the quantum dot to construct initial vectors and a preconditioner. We apply these to accelerate the convergence of the folded spectrum method for the interior states at the top of the valence and the bottom of the conduction band. For large CdSe quantum dots, the number of iteration steps until convergence decreases by about a factor of 4 compared to previous calculations.
Published by Elsevier Inc.

Keywords: Computational nano-technology; Electronic structure; Preconditioned conjugate gradients; Bulk band; Quantum dots

1. Introduction

A challenging task in computational nano-science is to predict electronic properties and their changes due to quantum confinement effects in experimentally synthesized nano-systems such as quantum dots.

One approach to large scale quantum dot calculations is to first construct the single particle Hamiltonian of the system either by the empirical pseudopotential or the charge patching method. Only a few of the interior eigenvalues on either side of the band gap are computed as they determine many of the optical and electronic properties of the system. These band edge states are solutions of an effective single particle Schrödinger equation

☆ This work was supported by the US Department of Energy under LAB03-17 initiative, Contract Nos. DE-FG02-03ER25584 and DE-AC03-76SF00098.

* Corresponding author. Tel.: +1 510 486 7691.
E-mail addresses: voemel@eecs.berkeley.edu, cvoemel@lbl.gov (C. Vömel), tomov@cs.utk.edu (S.Z. Tomov), LWWang@lbl.gov (L.-W. Wang), OAMarques@lbl.gov (O.A. Marques), dongarra@cs.utk.edu (J.J. Dongarra).

0021-9991/$ - see front matter Published by Elsevier Inc.
doi:10.1016/j.jcp.2006.10.005

$$H\Psi_i \equiv \left[-\frac{1}{2}\nabla^2 + V\right]\Psi_i = \epsilon_i \Psi_i, \tag{1}$$

see [12,13,16,20]. In (1), H represents the Hamiltonian, $\psi_i(r)$ denotes the single particle wave function with energy ϵ_i and V the potential. In contrast, in the self-consistent field (SCF) iteration [17,18], a large number of eigenstates of (1) need to be computed [21].

We apply the parallel energy SCAN (ESCAN) method [4,25] where a semi-empirical potential or a charge patching method [24] is used to construct V. In a plane wave basis, the Hamiltonian H is only implicitly available: the kinetic energy part is represented in Fourier space where it is diagonal, and the potential energy part is evaluated in real space (via the fast Fourier transformation, FFT) so that the number of calculations used to construct the matrix-vector product scales as $n\log n$ rather than n^2 where n is the dimension of H. To compute interior eigenstates close to a reference energy E_{ref}, we use the preconditioned conjugate gradient (PCG) [14,16] method with a spectral transformation, the *folded spectrum* approach [26]: the interior eigenvalue problem is transformed to find the smallest eigenvalues of

$$(H - E_{\text{ref}} I)^2 \Psi_i = \epsilon_i \Psi_i. \tag{2}$$

However, there can be convergence problems for large quantum dot systems with strongly clustered, nearly degenerate eigenstates. Squaring the Hamiltonian in (2) contributes to the stronger clustering of the eigenvalues and a decreased convergence rate of PCG.

This current work addresses these difficulties. The foundation of our approach lies in the observation that the converged quantum dot states around the band gap are confined to the interior of the quantum dot and are 'bulk-like'. We show how to make use of these cheaply computable bulk eigenstates [27] to improve the choice of the starting vector and the preconditioner for the quantum dot PCG eigensolver in ESCAN. We validate our approach on both CdSe bulk systems and colloidal quantum dots. From a physical point of view, CdSe quantum dots are one of the most thoroughly studied nanostructures because photoluminescence occurs at different frequencies, depending on the size of the dot. This property has many important practical applications such as optical tags in biological systems.

The rest of the paper is organized as follows. In Section 2 we explain the relationship between colloidal quantum dot and bulk band (BB) structure. The preconditioned conjugate gradient (PCG) method is explained in Section 3. Next, in Section 4, we show how to use bulk band information in the derivation of BB-type preconditioners for PCG. Section 5 contains our computational results. Finally, in Section 6, we state our conclusions and possible further extensions of this work.

2. Quantum dot and bulk band structure

The properties of ideal bulk systems such as crystals are well understood: their Bloch states can be computed relatively cheaply using direct G-space diagonalization when only a few atoms are in a unit cell. Colloidal quantum dots are more complicated physical objects where bulk materials and vacuum constitute the interior and exterior, respectively. Moreover, they usually are much larger, possibly consisting of thousands of atoms.

However, our key observation relating these two systems is that for large enough systems, the converged quantum dot states around the band gap have a *small* angle to the subspace defined by the corresponding bulk system states. This section describes the mathematical tools for relating the bulk and the quantum dot eigen-systems.

2.1. Quantum dot and BB space embedding

We first consider a bulk system on a primary cell with periodicities $\mathbf{a}_1$, $\mathbf{a}_2$, $\mathbf{a}_3$. The periodicity of the bulk in terms of this crystal unit corresponds to a periodic potential satisfying $V(\mathbf{r}+\mathbf{a}) = V(\mathbf{r})$. Bloch's theorem [1] states that the eigenstates $\Psi_{n\mathbf{k}}$ of the bulk Hamiltonian H are of the form

$$\Psi_{n\mathbf{k}}(\mathbf{r}) = u_{n\mathbf{k}}(\mathbf{r})e^{i\mathbf{k}\mathbf{r}}, \quad u_{n\mathbf{k}}(\mathbf{r}+\mathbf{a}) = u_{n\mathbf{k}}(\mathbf{r}). \tag{3}$$

The corresponding eigen-energies are denoted by $E_{n\mathbf{k}}$. From the expansion

$$u_{n\mathbf{k}}(\mathbf{r}) = \sum_{\mathbf{G}} c^{\mathbf{k}}_{n\mathbf{G}} e^{i\mathbf{G}\mathbf{r}}, \tag{4}$$

the **a**-periodicity of $u_{n\mathbf{k}}$ requires that

$$e^{i\mathbf{G}(\mathbf{r}+\mathbf{a})} = e^{i\mathbf{G}\mathbf{r}} \iff \mathbf{G} = \frac{2\pi}{a_1} j_1 \mathbf{b}_1 + \frac{2\pi}{a_2} j_2 \mathbf{b}_2 + \frac{2\pi}{a_3} j_3 \mathbf{b}_3, \quad j_{\{1,2,3\}} = \ldots, -1, 0, 1, \ldots \tag{5}$$

with $(\mathbf{b}_1, \mathbf{b}_2, \mathbf{b}_3) = (\mathbf{a}_1, \mathbf{a}_2, \mathbf{a}_3)^{-1}$.

To limit the computational effort, we only consider the truncated expansion

$$\Psi_{n\mathbf{k}}(\mathbf{r}) = \sum_{\mathbf{G}, |\mathbf{G}+\mathbf{k}| < q_{\text{cut}}} c^{\mathbf{k}}_{n\mathbf{G}} e^{i(\mathbf{G}+\mathbf{k})\mathbf{r}}, \tag{6}$$

with the **k** from the so-called first Brillouin zone (FBZ), see [1], and where q_{cut} refers to an energy cutoff.

Now consider the quantum dot in a supercell of extension **na**. The analogous periodicity argument requires the supercell solution to be of the form

$$\Psi(\mathbf{r}) = \sum_{\mathbf{q}} c_{\mathbf{q}} e^{i\mathbf{q}\mathbf{r}}, \tag{7}$$

where

$$e^{i\mathbf{q}(\mathbf{r}+\mathbf{n}\mathbf{a})} = e^{i\mathbf{q}\mathbf{r}} \iff \mathbf{q} = \frac{2\pi}{n_1 a_1} j_1 \mathbf{b}_1 + \frac{2\pi}{n_2 a_2} j_2 \mathbf{b}_2 + \frac{2\pi}{n_3 a_3} j_3 \mathbf{b}_3, \quad j_{\{1,2,3\}} = \ldots, -1, 0, 1, \ldots \tag{8}$$

defining the reciprocal space

$$S = \mathtt{span}\{e^{i\mathbf{q}\mathbf{r}} | \mathbf{q} \text{ satisfies (8)}\} \tag{9}$$

for the quantum dot.

In order to efficiently use bulk states for quantum dot computations, we choose only those **k** in (6) that satisfy

$$\mathbf{G} + \mathbf{k} = \mathbf{q}. \tag{10}$$

As a result,

$$\mathbf{k} = 2\pi \left(\frac{k_1}{n_1 a_1} \mathbf{b}_1 + \frac{k_2}{n_2 a_2} \mathbf{b}_2 + \frac{k_3}{n_3 a_3} \mathbf{b}_3 \right), \quad j_{\{1,2,3\}} = \ldots, -1, 0, 1, \ldots, \tag{11}$$

and **k** is in the FBZ.

We then define the bulk band (BB) space

$$S_{\text{BB}} = \mathtt{span}\{\Psi_{n\mathbf{k}} | \Psi_{n\mathbf{k}} \text{ from, (6) } \mathbf{k} \text{ satisfies (11)}\}. \tag{12}$$

With this definition, S_{BB} is a subspace of S (and usually of much smaller dimension).

The relationship between the different lattices is depicted in Fig. 1.

2.2. Low rank spectral approximation of the bulk Hamiltonian

One major goal of the current paper is to use the bulk Hamiltonian H_{BB} as a model for the quantum dot Hamiltonian and thus its inverse, for which a good approximation is relatively easy to compute, as a preconditioner for the quantum dot computation. This is plausible because the quantum dot wave functions near the band gap are localized *inside* the quantum dot where the quantum dot Hamiltonian is exactly H_{BB}.

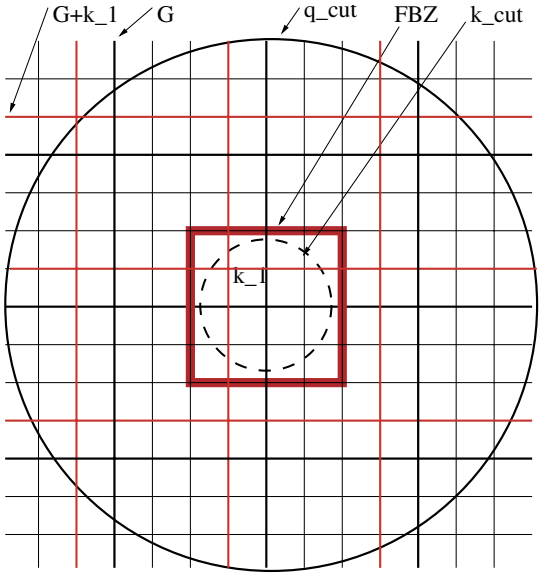

Fig. 1. Reciprocal space relationship: the sparse $\mathbf{G}+\mathbf{k}$-grid compatibly embedded into the $\mathbf{q}$-grid.

For purposes of preconditioning, we can represent the relevant part of the bulk Hamiltonian H_{BB} using its spectral decomposition into eigen energies E_{nk} and eigenstates Ψ_{nk} as given in (6).

If we just want to find the smallest eigenvalue of the original Hamiltonian from (1), we would use

$$H_{\mathrm{BB}}^{-1} \approx \sum_{n,k} \Psi_{nk} E_{nk}^{-1} \Psi_{nk}^{H}. \tag{13}$$

In preconditioning the folded spectrum Eq. (2), we use the analogous

$$(H_{\mathrm{BB}} - E_{\mathrm{ref}} I)^{-2} \approx \sum_{n,k} \Psi_{nk} (E_{nk} - E_{\mathrm{ref}})^{-2} \Psi_{nk}^{H}. \tag{14}$$

We make use of a low rank version, considering only a subset of states and selecting an energy cutoff, i.e. $n{:}n_{\min} \leqslant n \leqslant n_{\max}$, $k{:}|k| < k_{\mathrm{cut}}$.

3. The PCG algorithm

ESCAN uses the preconditioned conjugate gradient (PCG) method [25] with folded spectrum to compute interior eigenstates. The smallest eigenvalue λ of the Hermitian matrix $A \equiv (H - E_{\mathrm{ref}} I)^2$ (the one that corresponds to the eigenvalue of H closest to the reference point E_{ref}) minimizes the Rayleigh quotient

$$\lambda = \arg\min_{x \neq 0} \rho(x) \equiv \rho(x_j) = (x_j^H A x_j)/(x_j^H x_j). \tag{15}$$

From a current iterate x_j and a descent direction $d_j = -\nabla\rho(x_j) + \beta_j d_{j-1}$ [the (scaled) gradient being given by $\nabla\rho(x_j) = A\ x_j - x_j\rho(x_j)$] the method finds the angle

$$\theta_{j+1} = \arg\min_{\theta} \rho(x_j \cos\theta + d_j \sin\theta), \tag{16}$$

that is x_{j+1} minimizes the energy functional ρ in the two-dimensional subspace $\mathrm{span}\{x_j, d_j\}$. A preconditioner P can be used to influence the choice of the descent direction via

$$d_j = -P\nabla\rho(x_j) + \beta_j d_{j-1}, \tag{17}$$

see also [10,23]. After a number of band-by-band iterations, the Rayleigh–Ritz procedure is invoked to compute the best approximations from the subspace that the bands span, see also [15]. The procedure is summarized in Algorithm 1, for a more detailed discussion see the references in [14] and also [7,8,16].

4. Accelerating the nonlinear PCG algorithm

In this section, we discuss two complementary strategies to improve the folded spectrum PCG eigensolver in ESCAN for band gap calculations:

(1) Replace the random start vector by a (modified) bulk state at the gamma point, see Section 4.1.
(2) Replace the previously used preconditioner by one that better approximates the inverse of the bulk Hamiltonian, see Section 4.2.

Both approaches are motivated by the previously stated observation of a *small* angle between the quantum dot and the bulk system states close to the band gap.

4.1. Bulk-based starting vectors

While the Rayleigh–Ritz procedure on the complete bulk space S_{BB} is too expensive, it is still possible to find an inexpensive good initial vector for the PCG iteration. Experimentally, we found that the corresponding bulk wave function at the gamma point (the center of the first Brillouin zone [1]). constitutes an excellent starting vector for the PCG iteration.

From physics, it is known that the true solution we are looking for typically is confined to the interior of the quantum dot, see Fig. 2. We use the gamma point bulk state Ψ_{n0} and restrict it to the interior of the quantum dot in real space using a step mask function and setting it to zero outside the quantum dot.

Algorithm 1. The preconditioned conjugate gradient (PCG) algorithm for finding the *nstate* smallest eigenvalues of the operator $A = (H - E_{\mathrm{ref}}I)^2$.

Choose random start vectors X(1:nstate)
for i=1,niter **do**
  for m=1,nstate **do**
    Orthonormalize X(m) to X(1:m-1)
    $y_1 = A\ X(m)$ **for** j=1,nline **do**
      $\Lambda(m) = \rho(X(m)) = X(m)^H y_j$
      if state X(m) not yet converged **then**
        $r_{j+1} = (I - X(m)X(m)^H)y_j$
        $\beta = \frac{r_{j+1}^H Pr_{j+1}}{r_j^H Pr_j}$
        $d_{j+1} = (I - X(m)X(m)^H)(-Pr_{j+1} + \beta d_j), \gamma = \|d_{j+1}\|_2^{-1}$
        $e_{j+1} = A\ d_{j+1}$
        $\theta_{j+1} = 0.5\left|\arctan\left(\frac{2\gamma d_{j+1}^H y_j}{\Lambda(m) - \gamma^2 d_{j+1}^H e_{j+1}}\right)\right|$
        $X(m) = \cos(\theta_{j+1})X(m) + \sin(\theta_{j+1})\gamma d_{j+1}$
        $y_{j+1} = \cos(\theta_{j+1})y_j + \sin(\theta_{j+1})\gamma e_{j+1}$
      end if
    end for
  end for
  $[X(1{:}nstate), \Lambda(1{:}nstate)] =$ Rayleigh–Ritz on span $\{X(1{:}nstate)\}$
end for

4.2. The previously used preconditioner

In ESCAN, the preconditioners are designed to approximate $(H - E_{\mathrm{ref}}\, I)^{-2}$ in the case of solving the folded spectrum. The preconditioner that was used up to now in ESCAN is diagonal. It is applied in the Fourier space as

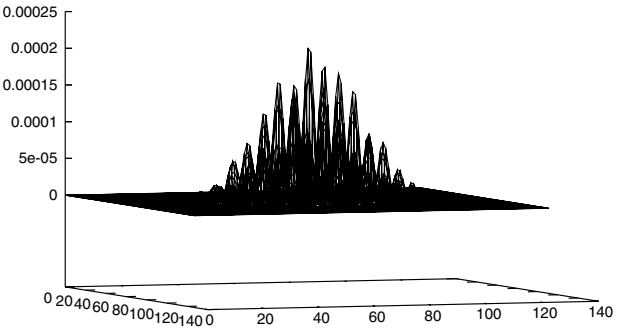

Fig. 2. Cross section of the charge density for the state at the top of the valence band (VBM). The wave-function is confined to the interior of the spherical CdSe quantum dot (which is centered in the middle of the box).

$$P^{-1} = D \equiv \left(I + \left(-\frac{1}{2}\nabla^2 + V_{\text{avg}} - E_{\text{ref}} \right) / E_k \right)^2 \tag{18}$$

where $-\frac{1}{2}\nabla^2$ is the Laplacian (diagonal in the Fourier space), E_{ref} is the shift used in the folded spectrum, V_{avg} is the average potential and E_k is the average kinetic energy of a given initial approximation of a wave function ψ_{init}, see [26].

4.3. New BB-type preconditioners

We describe how to improve the old preconditioner from (18). In order to use the approximation (14) from the bulk as preconditioner for the quantum dot, we use the L^2 projection Q^H of functions $R(r) \in S$ to S_{BB} (q-grid to G-grid), and Q to prolongate back from S_{BB} to S.

Using (12), we find

$$QQ^H \equiv \sum_{n:n_{\min} \leqslant n \leqslant n_{\max}, k:|k|<k_{\text{cut}}} \Psi_{nk} \Psi_{nk}^H \tag{19}$$

when only the states $n_{\min} \leqslant n \leqslant n_{\max}$ of S_{BB} are considered.

The residual R is decomposed into its S_{BB} and $S_{\text{BB}}^{\perp}$ components, i.e. $Q\,Q^H R$ and $R - Q\,Q^H R$. The S_{BB}-component is preconditioned with $(H_{\text{BB}} - E_{\text{ref}} I)^{-2}$, approximated by (14). The $S_{\text{BB}}^{\perp}$ component is preconditioned with the diagonal preconditioner D^{-1} from (18). In summary, the preconditioned residual is given by

$$PR \equiv Q(H_{\text{BB}} - E_{\text{ref}} I)^{-2} Q^H R + D^{-1}(R - QQ^H R). \tag{20}$$

4.4. Efficient implementation of the new preconditioner

As described in Section 2.1, the bulk wave functions are *sparse* vectors in the reciprocal space; the degree of sparsity depends on the supercell size.

The efficient application of the preconditioner in (20) relies on the implementation of (19), which involves

- the dot products $\alpha_{nk} \equiv \Psi_{nk}^H R$ between distributed vectors, R being dense and Ψ_{nk} being sparse, and
- the sum $\sum \alpha_{nk} \Psi_{nk}$ of scalar multiples of distributed sparse vectors.

For each sparse wave function, we use an integer array Q_LOCAL to store the indices of the local Fourier coefficients in compressed form. These are computed once at the beginning of the program and subsequently used as indirect addresses; they are the same for the Ψ_{nk} of all states n but depend on the k-point k. The following Algorithm 2 is designed to reuse them as much as possible and to reduce the amount of global communication. For this reason, all dot products are performed locally first using a workspace array DOTP and then a single blocked ALL_REDUCE operation is performed to find all global dot products simultaneously.

Algorithm 2. Implementation of the preconditioning operation $P = Q\ Q^H R$.

Compute local dot products with distributed Ψ_{nk} for all bulk states.
Set array DOTP=0
for k=1,nk (nk=number of bulk k-points) **do**
  for g=1,ng(k) (ng(k)=local number of g points for this k-point) **do**
    q=Q_LOCAL(g)
    for n=1,nbulk (nbulk=number of bulk states) **do**
      $DOTP(n,k) = DOTP(n,k) + (\Psi_{nk}(g))*R(q)$
    end for
  end for
end for
Perform one blocked ALLREDUCE to sum up all local dot products.
DOTP=GLOBAL_SUM(DOTP)
Compute projection P, a scaled sum of sparse vectors.
P=0
for k=1,nk **do**
  for g=1,ng(k) **do**
    q=Q_LOCAL(g)
    for n=1,nbulk **do**
      $P(q) = P(q) + \Psi_{nk}(g)DOTP(n,k)$
    end for
  end for
end for

5. Numerical results

We present two different experimental evaluations of our proposed modifications in ESCAN. We first validate the preconditioner on bulk systems, see Section 5.1. We then show, in Section 5.2, the impact of an improved initial vector and new preconditioner on large CdSe quantum dots. The experiments were performed on the IBM SP seaborg.nersc.gov consisting of Power 3 processors with a peak performance of 1.5 GFlops. The processors are distributed among 380 compute nodes with 16 processors per node.

5.1. Validation of the preconditioner on a bulk system

For the bulk problems, we start with a randomly generated initial guess and show the convergence history on two CdSe bulk systems consisting of 64 and 512 atoms, respectively.

The convergence histories for the two test systems are given on Fig. 3. We solve for the 4 lowest eigen-states and the convergence shown is for one of the three degenerate VBM states. The required accuracy is residual in L^2 norm to be less than 10^{-10}. We get convergence using the new preconditioner in 3 and 4 iterations for correspondingly the first and second test systems. For test system 2 the new method reduces the number of iterations by a factor of 4.

5.2. CdSe quantum dot problems

We consider two large CdSe quantum dots that are described in Table 1 and compute the three degenerate states at the top of the valence band using PCG with folded spectrum.

The results are summarized on Fig. 4. We compare three methods, the old preconditioner with random start vector, and old and new preconditioner with improved start vector. The combined improvements not only result in a significant reduction in the number of iterations, they also enable faster convergence to a small

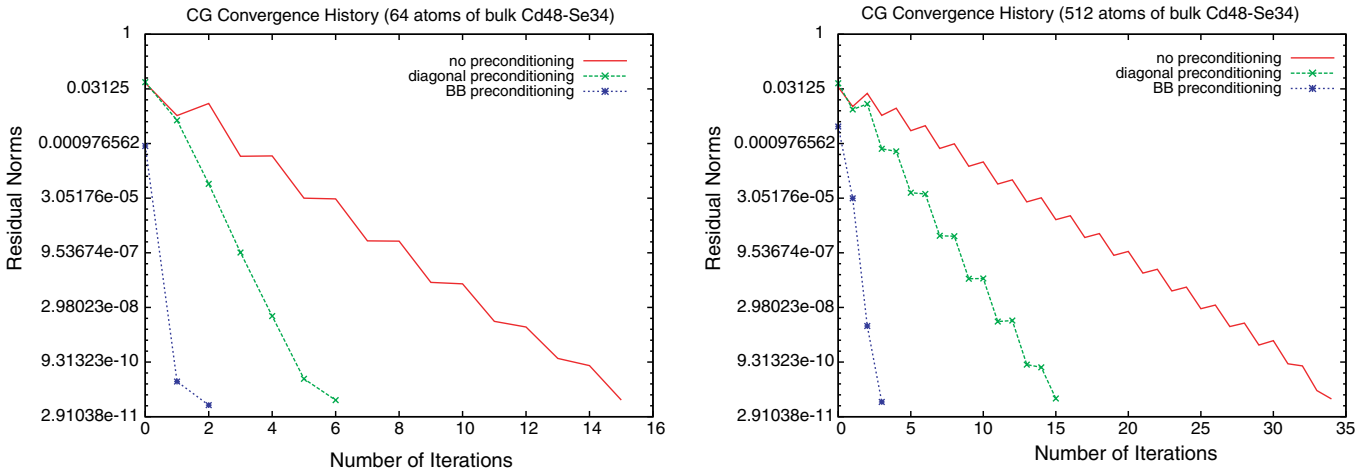

Fig. 3. Convergence histories for bulk test systems (left: 64 atoms, right: 512 atoms) as described in Subsection 5.1. Shown are the convergence without preconditioner, with diagonal preconditioner, and with BB preconditioner.

Table 1
Quantum dot considered in the comparisons in Fig. 4 and the dimensions of the BB subspace S_{BB}

Quantum dot size (atoms)	Grid size (real space)	System size (plane wave)	BB states (n,k)	Angle VBM to S_{BB}
784 Cd, 739 Se	128^3	145K	(5949)	2.3°
1568 Cd, 1601 Se	160^3	282K	(5949)	1.9°

The last column shows the angle between the converged VBM wave function and its projection on the space S_{BB}.

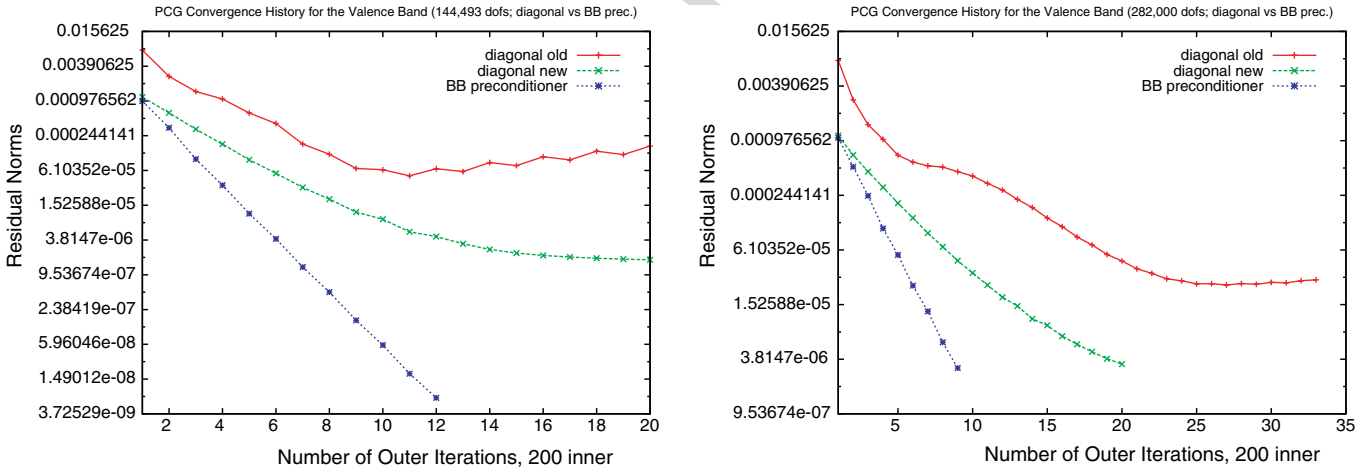

Fig. 4. Comparison of diagonal preconditioner (with random and improved initial vector) and BB preconditioner with improved initial vector. Shown is the convergence for one of the three degenerate VBM states with the folded spectrum approach for the two quantum dots from Table 1. The left and right picture show the convergence for the $Cd_{784}Se_{739}$ and Cd_{1568} Se_{1601} quantum dots, respectively.

residual norm. The speedup over the old preconditioner with improved initial vector is at least a factor of two. The speedup is much larger compared to the old preconditioner with random start vector where the convergence tends to stagnate at a certain level.

Note that while the convergence results are displayed as a function of the number of iterations, the picture is the same for the computing time. Using the implementation described in Section 4.4, the overhead for using the new preconditioner is less than 5% compared to using the old one and does not impact the scalability of the underlying code [4].

6. Conclusions and possible extensions

In this paper, we presented a bulk-based acceleration for computing interior states close to the band gap of colloidal quantum dots. By the example of large CdSe quantum dots, we showed a significantly faster and more accurate computation of the band edge states. An extension to other systems such as GaAs quantum dots is possible.

Acknowledgments

This work was supported by the US Department of Energy, Office of Science, Office of Advanced Scientific Computing (MICS) and Basic Energy Science under LAB03-17 initiative, contract Nos. DE-FG02-03ER25584 and DE-AC03-76SF00098. We also used computational resources of the National Energy Research Scientific Computing Center, which is supported by the Office of Science of the US Department of Energy. We thank the referee for comments that improved this paper.

References

[1] N.W. Ashcroft, N.D. Mermin, Solid State Physics, first ed., Saunders College, Philadelphia, 1976.
[4] A. Canning, L.-W. Wang, A. Williamson, A. Zunger, Parallel empirical pseudopotential electronic structure calculations for million atom systems, J. Comp. Phys. 160 (2000) 29–41.
[7] A. Edelman, T.A. Arias, S.T. Smith, The geometry of algorithms with orthogonality constraints, SIAM J. Matrix Anal. Appl. 20 (2) (1999) 303–353.
[8] A. Edelman, S.T. Smith, On conjugate gradient-like methods for eigen-like problems, BIT 36 (3) (1996) 494–508.
[10] A. Knyazev, Preconditioned eigensolvers – an oxymoron? Electr. Trans. NA 7 (1998) 104–123.
[12] W. Kohn, L.S. Sham, Self-consistent equations including exchange and correlation effects, Phys. Rev. 140A (1965) 1133–1140.
[13] C. Le Bris, P.-L. Lions, From atoms to crystals: a mathematical journey, Bull. Am. Math. Soc. 42 (3) (2005) 291–363.
[14] J. Nocedal, S.J. Wright, Numerical Optimization, 1st ed., Springer, New York, 1999.
[15] B.N. Parlett, The Symmetric Eigenvalue Problem (Classics in Applied Mathematics), SIAM, Philadelphia, 1998.
[16] M.C. Payne, M.P. Teter, D.C. Allan, T.A. Arias, J.D. Joannopoulos, Iterative minimization techniques for ab initio total-energy calculations: molecular dynamics and conjugate gradients, Rev. Mod. Phys. 64 (1992) 1045–1097.
[17] P. Pulay, Convergence acceleration of iterative sequences. The case of SCF iteration, Chem. Phys. Lett. 73 (2) (1980) 393–398.
[18] P. Pulay, Improved SCF convergence acceleration, J. Comp. Chem. 3 (4) (1982) 556–560.
[20] Y. Saad, J.R. Chelikowsky, S.M. Shontz. Numerical methods for electronic structure calculations of materials. Technical Report umsi-2006-15, University of Minnesota, Department of Computer Science and Engineering, March 2006.
[21] Y. Saad, A. Stathopoulos, J.R. Chelikowsky, K. Wu, S. Ogut, Solution of large eigenvalue problems in electronic structure calculations, BIT 36 (3) (1996) 1–16.
[23] Z. Bai, J. Demmel, J. Dongarra, A. Ruhe, H. van der Vorst (Eds.), Templates for the Solution of Algebraic Eigenvalue Problems: A Practical Guide, SIAM, Philadelphia, 2000.
[24] L.W. Wang, J. Li, First principle thousand atom quantum dot calculations, Phys. Rev. B 69 (2004) 153302.
[25] L.-W. Wang, A. Zunger, Solving Schrödinger's equation around a desired energy: application to silicon quantum dots, J. Chem. Phys. 100 (3) (1994) 2394–2397.
[26] L.-W. Wang, A. Zunger, Pseudopotential theory of nanometer silicon quantum dots application to silicon quantum dots, in: P.V. Kamat, D. Meisel (Eds.), Semiconductor Nanoclusters, Elsevier Science, Amsterdam, Netherland, 1996, pp. 161–207.
[27] L.-W. Wang, A. Zunger, Linear combination of bulk band method for strained system million atom nanostructure calculations, Phys. Rev. B 59 (1999) 15806.